CHAPTER III

CHARACTERIZATIONS OF THIN FILM

In this chapter, the characterization techniques of thin films that have been used in this work will be described. Thin films are characterized for their structural and tribological properties. For the structural properties of the thin films, the crystallinity can be analyzed by X-ray diffraction method. In addition, scanning electron microscopy with energy dispersive X-ray analysis is used to determine the chemical composition of the films. Using the atomic force microscope and scanning tunneling microscope investigate the morphology of the films. For the tribological properties, hardness, friction coefficient and wear rate can be calculated from the atomic force microscope with nanoindentation attachment.

3.1 X – Ray Diffraction

X – Ray diffraction (XRD) is a non-destructive technique for identifying the crystalline phase in materials and investigating the structural properties such as preferred orientation and defect structure. Figure 3.1 shows the diffraction of X-ray from parallel planes in the crystal followed by Bragg law. The monochromatic X-ray beam with a specific wavelength is projected on the lattice plane at an angle theta (θ). And then, the X-ray beam is diffracted from planes in the specimen. The diffraction condition can be occurred by according to Bragg's law.

$$2d\sin\theta = n\lambda, \qquad (3.1)$$

when d is a spacing between atomic planes in the crystal,

λ is wavelength of x- ray beam,

θ is the Bragg angle for an incident angle as same as a diffracted angle.

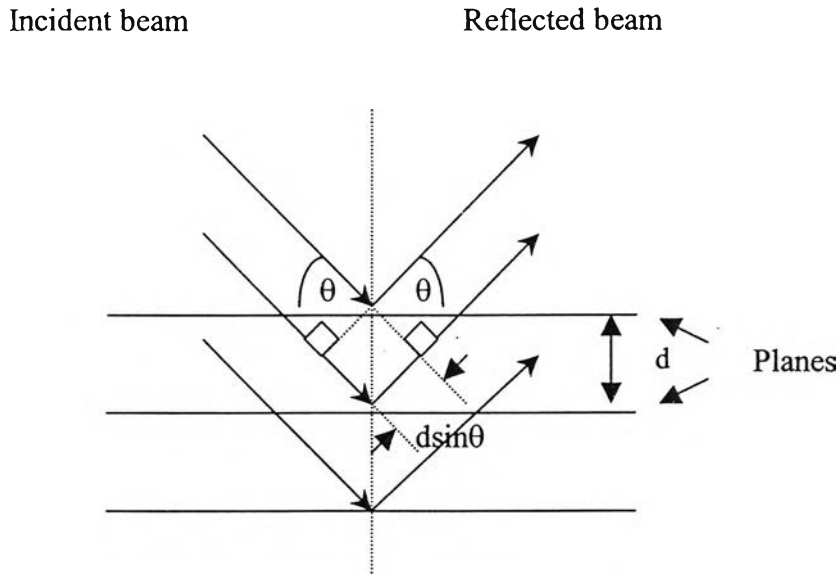

Figure 3.1: Diffraction of X- ray from parallel planes in the crystal followed by Bragg law

In this work, the structural information can be investigated by using $2\theta - \omega$ scan method.

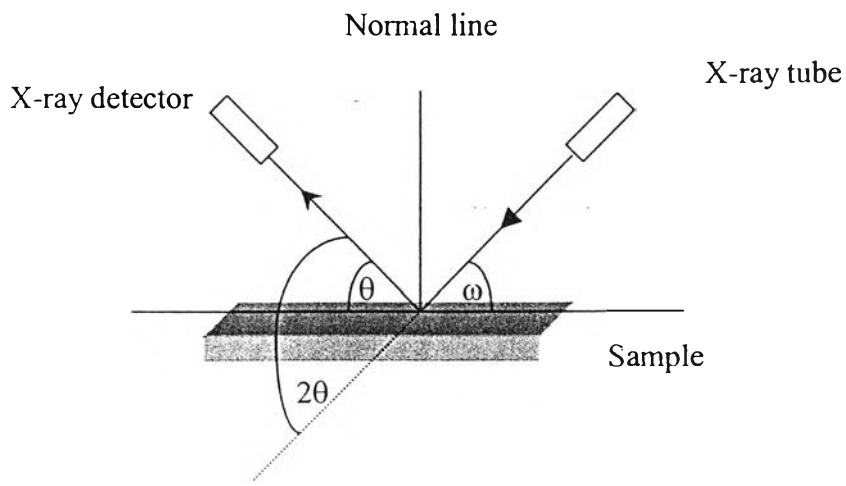

Figure 3.2: Basic features in XRD experiment

where ω is an angle between an incident beam and a sample,

2θ is an angle between an incident beam and an reflected beam.

As shown in Figure 3.2, the incident angle ω is not equal to the diffraction angle (θ). The X-ray tube and the detector are moved in varying the angle ω and θ respectively, while the sample is fixed. And then the intensity of the diffraction of X-ray is measured as a function of the diffraction angle (2θ). This mode can be used to determine the phase and the preferred orientation. If ω is equal to theθ, this scan mode is known as $2\theta - \theta$ scan.

3.1.1 Peak Broadening

A width of intensity peak in $\omega - 2\theta$ X–ray scan can be used as an indicator of a mosaicity of film. It is occurred due to an imperfect of the crystal. In this case, a single crystal is broken up to a number of tiny blocks. Each block slightly disorient from others, as shown in Figure 3.3 [32]. This phenomenon makes the x-ray peak more broadening for crystalline thin film than that for perfect crystal. In addition, the peak width can be referred the crystal quality of the thin film. The wider of the peak width makes the lower crystallographic order in layers. This phenomenon makes the crystal quality is lower. In case of the crystal quality, it depends on a variation in d spacing. If the d - spacing between the lattice planes is equal, the film will has high quality.

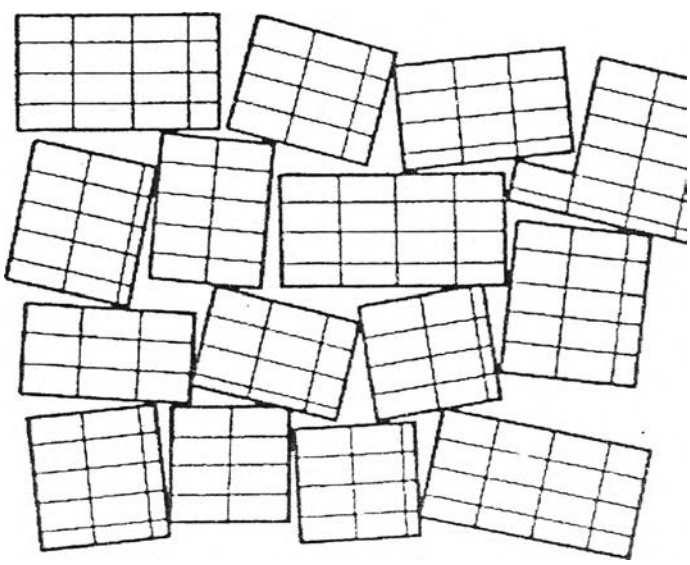

Figure 3.3: Mosaic structure of real crystal [32]

3.2 Scanning Tunneling Microscope

Scanning tunneling microscope (STM) is used to obtain images of surface at an atomic scale. The schematic of the scanning tunneling microscope is shown in Figure 3.4.

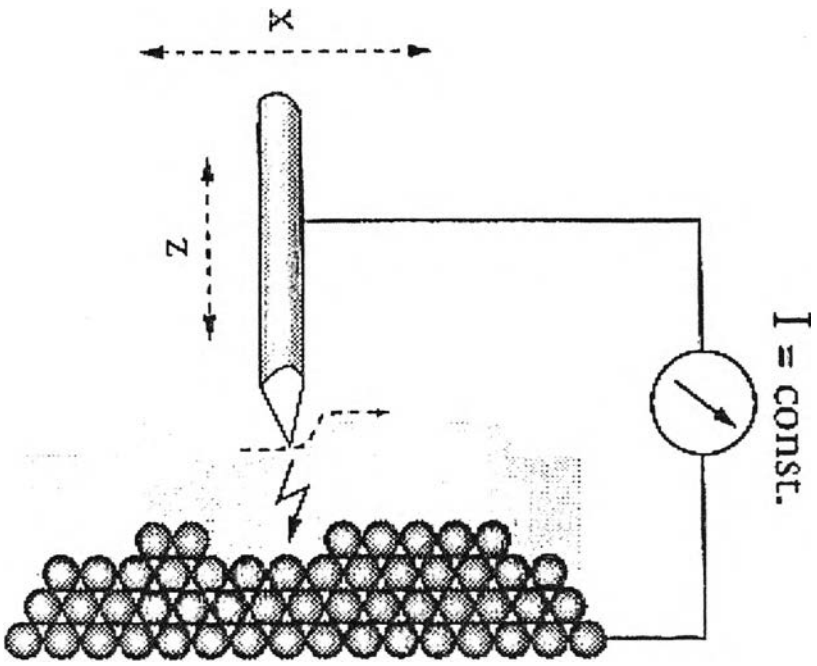

Figure 3.4: Schematic of the scanning tunneling microscope [33]

The distance between a tip and the sample surface is so small about 1 nm. If low voltage (~0.1 V) is applied between the tip and the sample surface, small current will flow between them. This is the tunneling current. The Sommerfeld's model can be used to explain this process, as shown in Figure3.5 (a). The gap between the tip and the surface is *d*. If electrons want to move from the sample to the tip, they will be acquired the energy more than the work function of the sample (ϕ). When the voltage

is applied, the electronic structure is changed, as shown in Figure 3.5 (b). In quantum mechanics, the electrons can go through the gap to the tip. This phenomenon produces the tunneling current. This current depends on the tip-sample separation distance, the bias voltage and the work function. This relation is shown in following equation [34]

$$I = keV \exp[-2\frac{\sqrt{2m\phi}}{\bar{h}}d], \qquad (3.2)$$

where k is constant,

e is electron charge,

h is Planck' constant,

d is the tip – sample separation distance,

V is the bias voltage between tip and sample,

ϕ is the work function of the sample,

m is the electron mass,

I is the tunneling current.

From the equation (3.2), the current decreases exponentially in the distance between the tip and the sample, as the distance increases. In this work, a small sharp tungsten tip is scanned over the sample surface and the distance is kept constant. The current is also kept constant. As a result, the tip follows the structure of the surface. During the scanning, the movement of the tip is recorded and a topographic image is generated and showed on the computer screen line by line. STM can be used to obtain image of conductor and semiconductor samples.

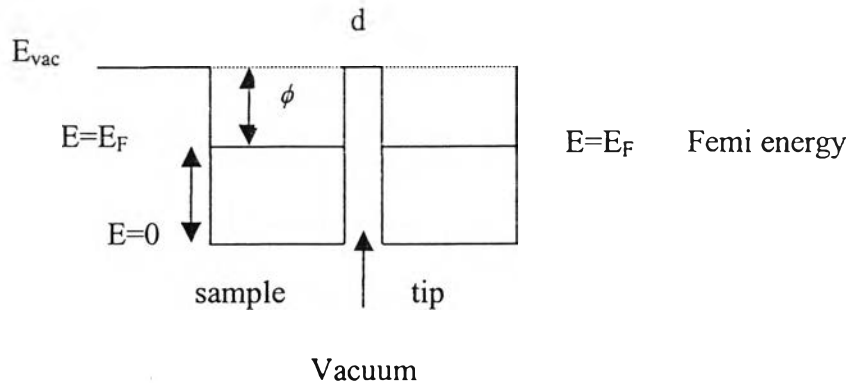

a) bias voltage (V) = 0

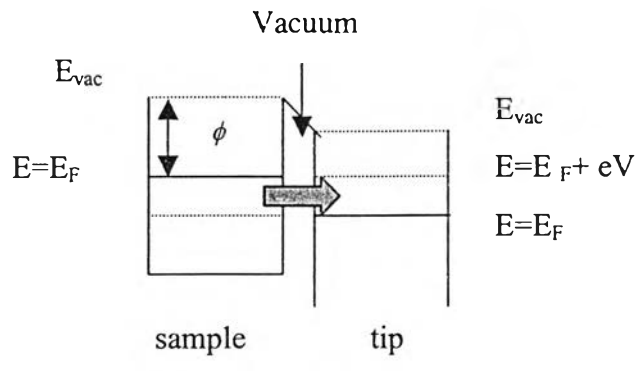

b) bias voltage (V) ≠ 0

Figure 3.5: Diagram of electron tunneling current a) bias voltage (V) = 0 and b) bias voltage (V) ≠ 0

3.3 Atomic Force Microscope

Atomic force microscope (AFM) is used to obtain the image and surface information similar to STM. However, there are some differences in signal and processing image. The image of AFM is produced van der waals force that is the interaction between the sample surface and a tip on cantilever. The tip of AFM is located at the end of cantilever and scans over the surface, as shown in Figure 3.6.

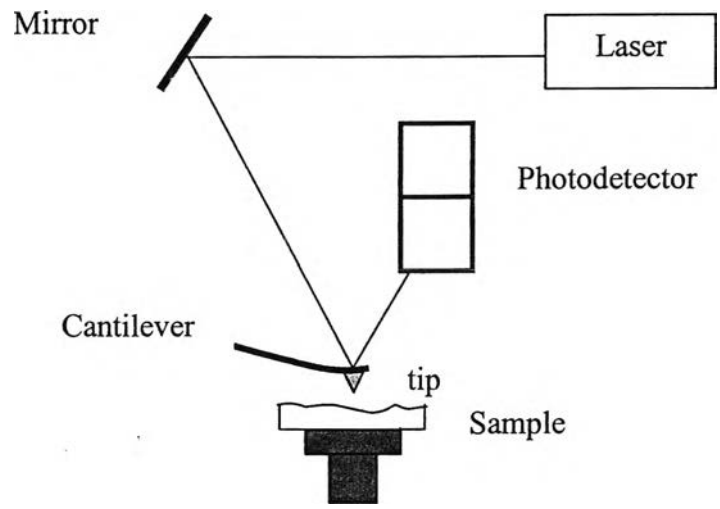

Figure 3.6: Schematic of atomic force microscope

A beam of laser is reflected from cantilever to a photodetector that measures the cantilever deflection. Then, the signal is transformed to create an image of surface. Because the tip and cantilever are flexible, Hooke's law can be used to describe the force that happens while the tip scans over the surface.

$$F = -kz\,, \tag{3.3}$$

where F is the force,

k is the spring constant of the cantilever,

z is the displacement of the cantilever.

In this work, "*Tapping mode*^{TM}" AFM is used. A Si tip slightly taps on the sample surface during scanning. In this process, the oscillation amplitude of the cantilever is constant. So, the tip – sample interaction is constant. An advantage of this mode is that the tip is less damage from the contact between the sample and tip than other modes. AFM can be used to obtain image of almost all samples, including insulators, semiconductors and conductors. The surface information such as root mean square (RMS) surface roughness can be calculated from AFM analysis. RMS roughness is a standard deviation of the surface height within a given area [35].

$$RMS = \sqrt{\frac{\sum_{i=1}^{N}(Z_i - Z_{ave})^2}{N}}, \qquad (3.4)$$

where Z_{ave} is the average surface height within the given area,

Z_i is the current surface height,

N is the number of point within a given area.

For investigation hardness of the thin films, the nanoindentation of AFM is used. In this mode, a Si tip is changed to a diamond tip. This diamond tip is located at the end of metal cantilever. This tip is forced into the sample surface and then it is retracted from the surface and makes an indent on the surface, as shown in Figure 3.7.

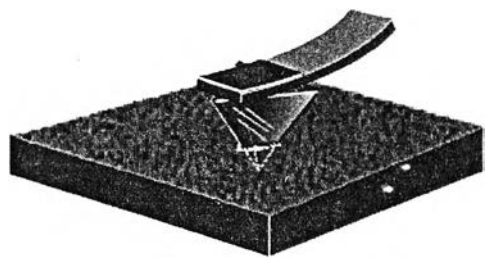

a)

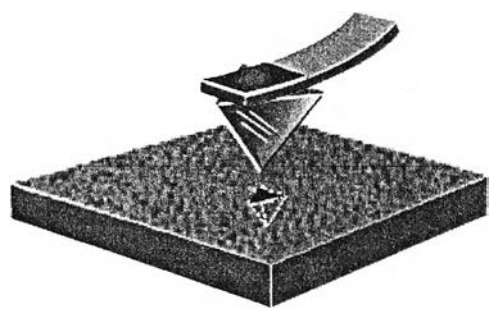

b)

Figure 3.7: Nanoindentation process a) indentation the diamond tip into the surface b) the indent on the surface after retracing the diamond tip [35]

The hardness of thin film (H) can be calculated from the indent. From the relation

$$H = \frac{F}{A}, \tag{3.5}$$

and

$$A = \frac{3\sqrt{3}\tan a}{\cos a} h^2, \tag{3.6}$$

where F is the test force,

A is the surface area of the indenter that penetrates beyond the surface surface,

h is a penetrate depth,

a is the face angle (60°).

In this work, the geometry of diamond tip is a three-sided pyramid (plus the bottom) with an apex angle of about 60°. During the nanoindentation, the graph between tip deflection and distance of the scanner movement in z direction is recorded and shown as Figure 3.8.

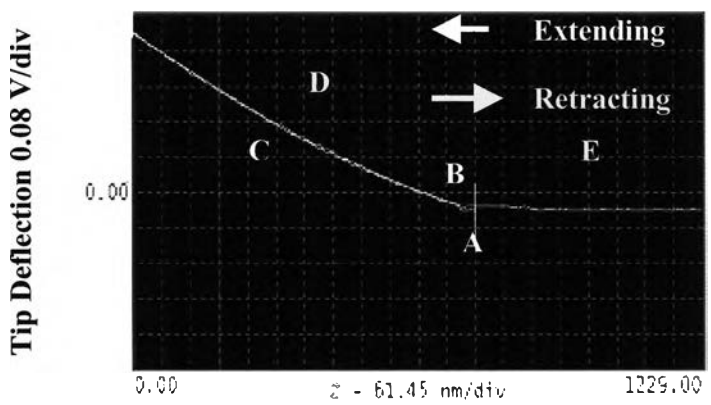

Figure 3.8: AFM force plot of the diamond tip probe on the thin film for nanoindentation

A force curve plots the deflection of the force-sensing cantilever as the tip is extended toward the sample (white line) and retracted from the sample (yellow line). In this method, the tip is fixed while the sample contact with the scanner is moved toward the sample. Several points along the force curve are shown in Figure 3.9.

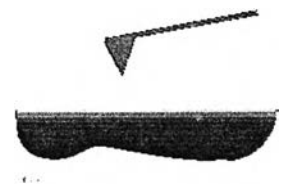

A) Non-contact region

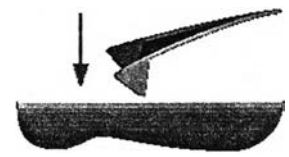

B) Jump to contact

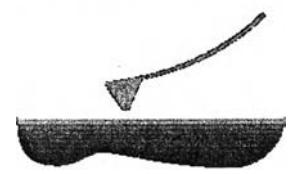

C) Contact

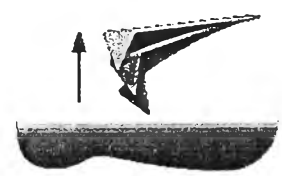

D) Pull off

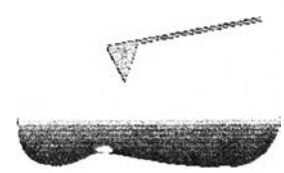

E) Non-contact region

Figure 3.9: Schematic of cantilever–sample interaction at several points along the force curve [35]

The cantilever movement starts at point A. In this point, there is no contact between the tip and the sample surface. So, this part of the force curve shows no deflection. As the tip is very close to the surface, it may jump to the surface because of the sufficient attractive force between the tip and the sample. When the tip is in contact with the surface and indent into the surface, the cantilever deflection increases, as shown in section C. After the cantilever loads to the desired force value, it unloads from the sample. This phenomenon makes the cantilever deflection decrease until the tip and the sample surface don't contact each other, as shown in section D. When there is no contact between the tip and the sample surface, the force curve shows no deflection as shown in section E.

For nanoindentation, there is no feedback to control the force or displacement. Only a maximum cantilever deflection is controlled. As a result, the maximum deflection of load is the same as those of unload.

The force can be calculated from [35]

$$F = kVS, \tag{3.7}$$

where k is the spring constant of cantilever (N/m),

V is the trigger threshold (V),

S is the deflection sensitivity (m/V).

For investigation the friction coefficient and wear rate of thin films, the scratch mode in AFM was used. In this mode, the diamond tip scratches into the sample surface and then the tip is taken away from the surface. The wear groove appears on the surface, as shown in Figure 3.10.

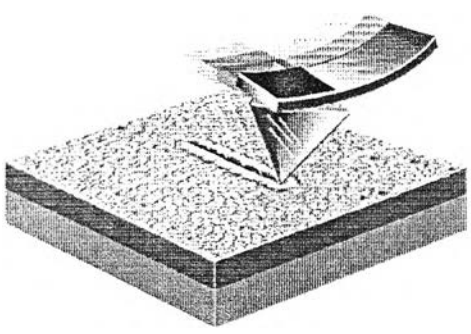

Figure 3.10: Nanoscratching consists of moving a diamond tip through the sample [35]

The force plot in this mode cannot show the force and displacement during the scratch. In contrast, the force plot shows the deflection of tip at the start and the end of the scratch. During the scratch, the friction force is created between the tip and the surface. So, the maximum deflection of cantilever after scratching is larger than that of cantilever before scratching, as shown in Figure 3.11.

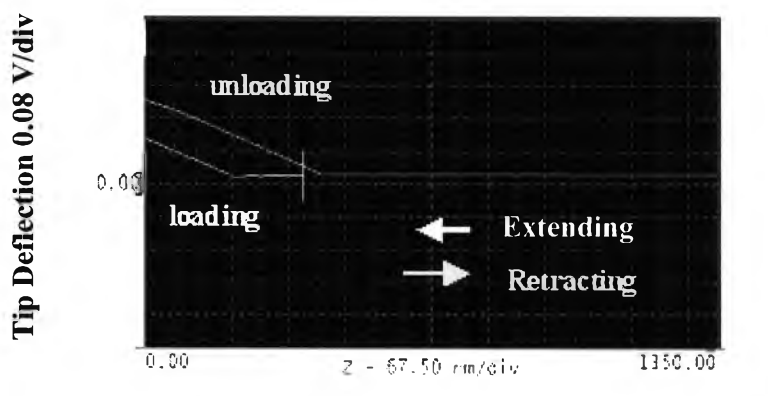

Figure 3.11: AFM force plot of the diamond tip AFM probe on the thin film for nanoscratching

The force curve plots the deflection of the force-sensing cantilever as the tip is extended toward the sample (white line) and retracted from the sample (yellow line).

Figure 3.12 shows the diagram of forces that act at the diamond tip [36]. For ideal indentation, the normal force (P) is only one force that acts at the diamond tip. This force makes the movement of the tip in vertical displacement shown in Figure 3.12(a). A bending of cantilever makes a lateral displacement of the tip. So, the lateral force, F_L is occurred from the movement of the tip. For correction this force, a compensating lateral motion of probe is controlled by the AFM software. From the motion of the probe, the force that acts on the tip in horizontal direction is called a compensating force, F_C, as seen in Figure 3.12(b). As the lateral force and the compensating force are equal in magnitude and opposite in the direction, the net force in horizontal direction is zero. The result is the same as idealized indentation. In

practice, the lateral compensation is controlled to minimize uncertainties and additional moment term at the end of the cantilever. During the scratch test, the friction force occurs due to the movement of the tip into the sample surface, as in Figure 3.12(c). The difference between F_L and Fc is assumed to cancel. So, the friction force is the one force that acts at the tip. This force causes the moment of the friction force (M_f) around the end of the cantilever. This moment cannot occur for the indentation. In addition, this moment causes larger cantilever deflection after scratching. The moment of the friction force can be calculated from

$$M_f = fd_2, \tag{3.8}$$

where f is the friction force,

d_2 is the distance between the tip and the end of the cantilever.

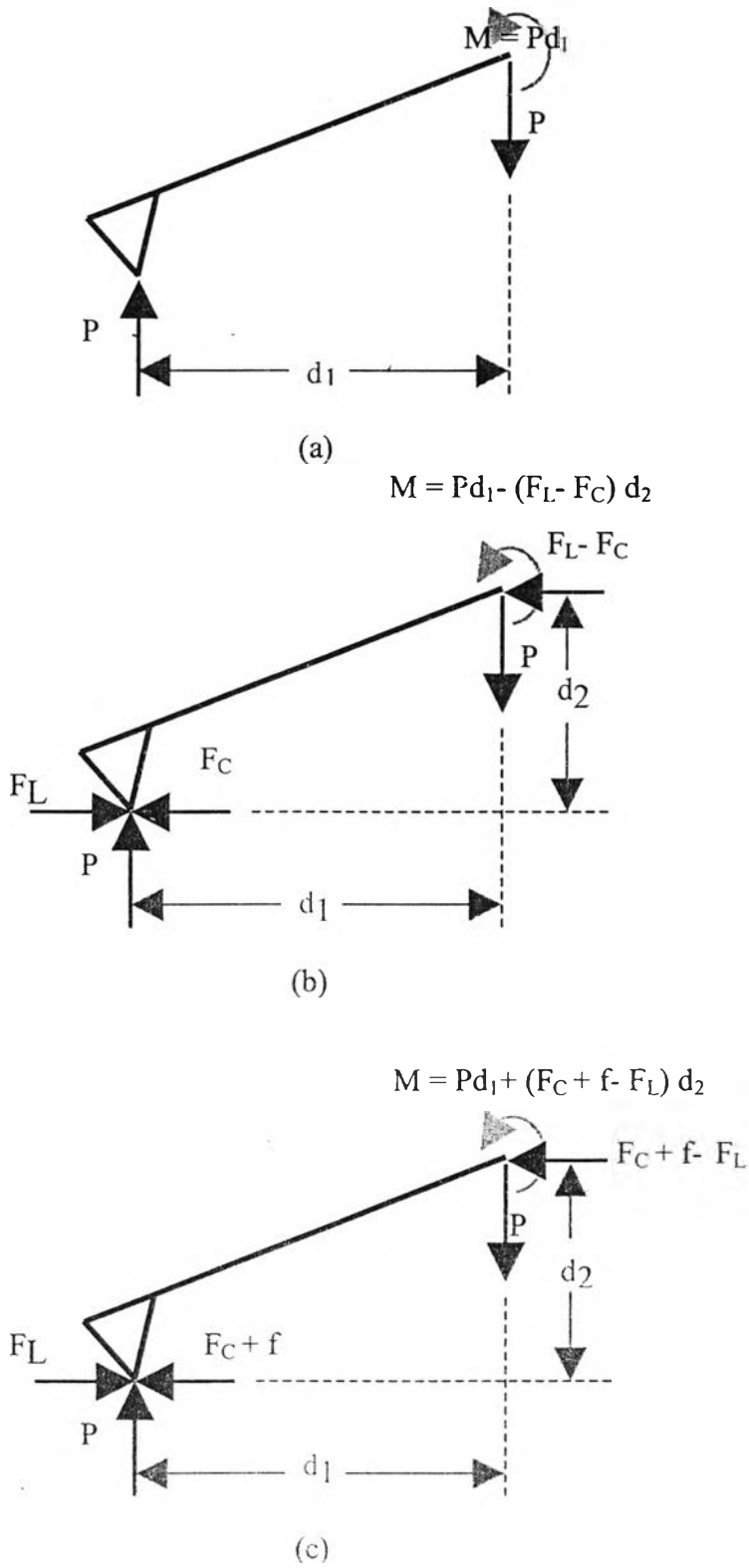

Figure 3.12: Diagrams of the AFM cantilever probe for (a) idealized indentation, (b) indentation testing (c) nanoscratch testing with a scratch angle of 0° [36]

To determine the friction force, the difference between the force at the start and the end of the scratch (ΔP) in force curve for nanoscratching is considered.

$$M_f = \Delta P d_1 = f d_2, \qquad (3.9)$$

where d_1 is the horizontal distance between the tip and the end of the cantilever.

The distance of d_1 and d_2 can be calculated from a geometry of the cantilever and tip. In this work, an angle of the cantilever is 12°, a length and a thickness of the cantilever are approximately 350 and 13 μm, respectively. A height of the diamond tip is 100 μm, as illustrated in Figure 3.13. Using these probe dimensions, d_1 and d_2 are calculated to be 264 and 173 μm, respectively. For calculation d_1 and d_2, the thickness of the cantilever is canceled.

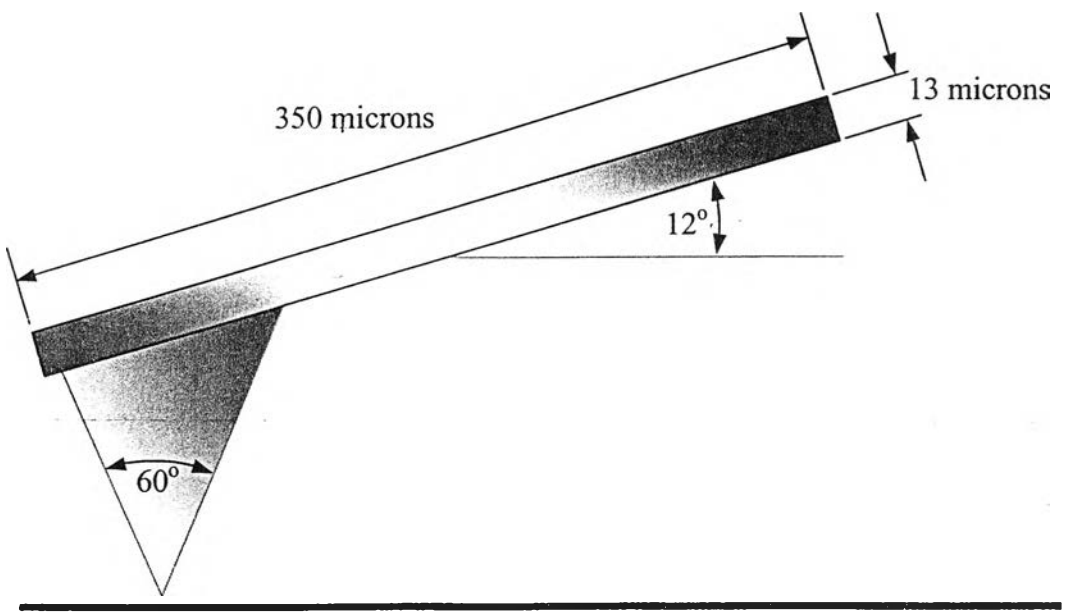

Figure 3.13: Typical indentation cantilever with dimensions

In the scratch test, the diamond tip makes the wear groove into the surface. The wear rate can be calculated from [1]

$$K_e = \frac{V}{FL} = \frac{A_v L}{FL} = \frac{A_v}{F}, \tag{3.10}$$

where V is the volume of material removed,

F is the normal load applied to the sample,

A_v is the cross sectional area of the wear groove,

L is the distance of the scratch.

To determine wear rate, a line scan cross sectional profile of scratch is used (see in Figure 3.14).

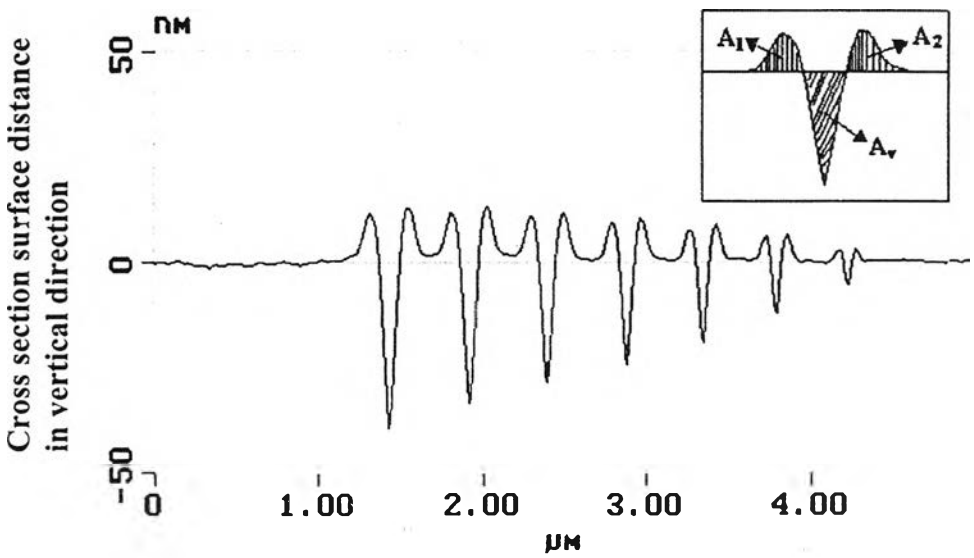

Figure 3.14: Cross sectional profile of the scratch using the AFM topographic data [36]

For the friction coefficient, it can be calculated from the relation between the friction force and the normal force that occur at the diamond tip during the scratch test. This relation is shown in the following equation

$$f = \mu N, \qquad (3.11)$$

when f is the friction force,

μ is the friction coefficient,

N is the normal force applied to the tip.

3.4 Scanning Electron Microscopy with Energy Dispersive X-ray Analysis

In Scanning Electron Microscope (SEM) with analytical electron microscope, a solid specimen is bombarded in vacuum by a primary electron beam. The interaction between a primary electron beam and a specimen creates various signals; for example, secondary electrons, backscattered electrons, transmitted electrons, X- ray, cathodoluminescence and Auger electrons, as shown in Figure 3.15 [37].

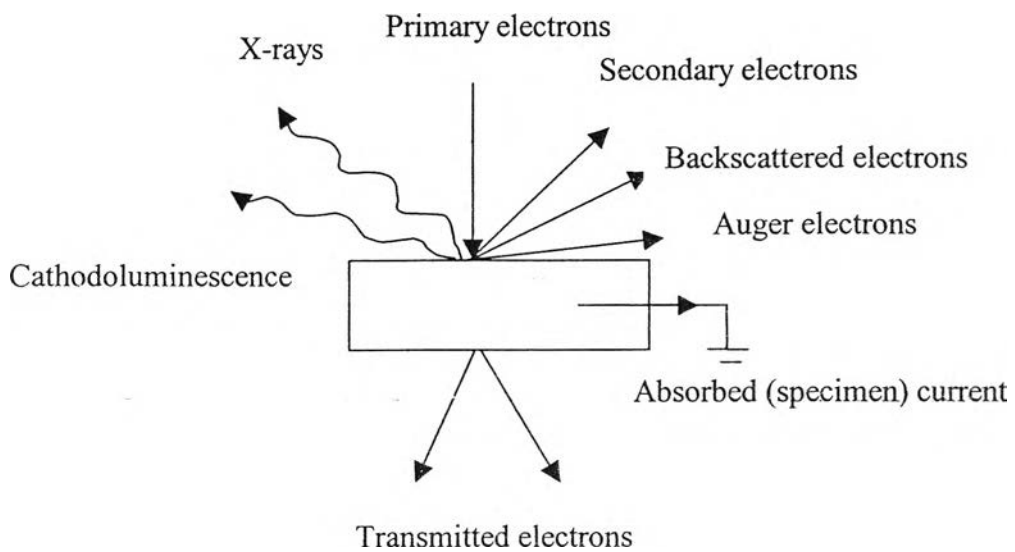

Figure 3.15: Photon and charged particle emission from an electron-bombarded surface

When the interaction is occurred, most of electrons come to rest within the droplet shaped volume that is elongated for the lower atomic mass (Z) and squashed for the higher atomic mass (Z) of the specimen, as shown in Figure 3.16. Within this

excitation volume, free electrons and the electromagnetic radiation are produced. For information of the microstructure, the secondary electrons are detected.

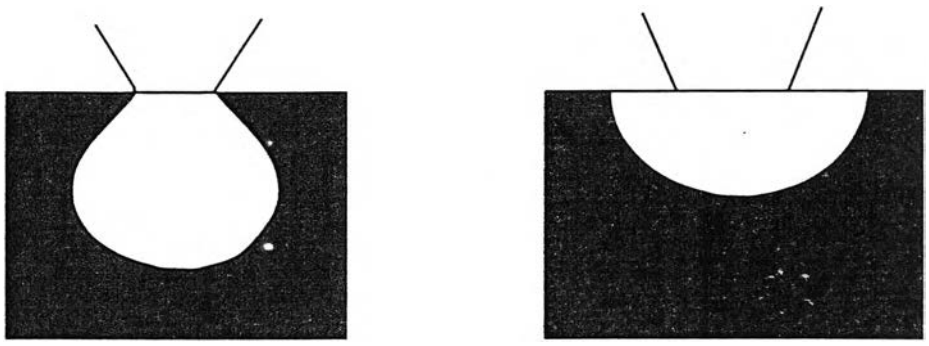

a) low atomic number b) high atomic number

Figure 3.16: Schematic showing the excitation volume [38]

The secondary electrons are created within 10 nm near the specimen surface and they have less kinetic energy than 50 eV. These electrons occur from the inelastic collision between the primary electrons and the specimen. These collisions make the outermost electron of atoms in the specimen be detached, and the atoms are ionized to be positively charged. These secondary electrons are emitted from the surface to vacuum and then they are captured to create a surface picture by a detector.

In this work, X-ray spectroscopy that is known as Energy Dispersive X-ray spectroscopy, EDS or EDX, is used to determine the chemical composition of the specimens by detecting characteristic X-ray. The emission of the characteristic X-ray process is shown in Figure 3.17. As a primary electron bombards the specimen, the inelastic collision between a core electron in the innermost shell such as K shell and a secondary electron is occurred. If the primary electron has more energy than the binding energy of electron in K shell, the core electron will be ejected from the atom. Then, a vacancy in the K shell is filled by an electron in higher energy level such as L, M shell. During the transition, the characteristic X- ray is radiated. The energy of X-

ray is the same as the difference of binding energy between two shells. In this case, K_α and K_β are emitted from the specimen, respectively.

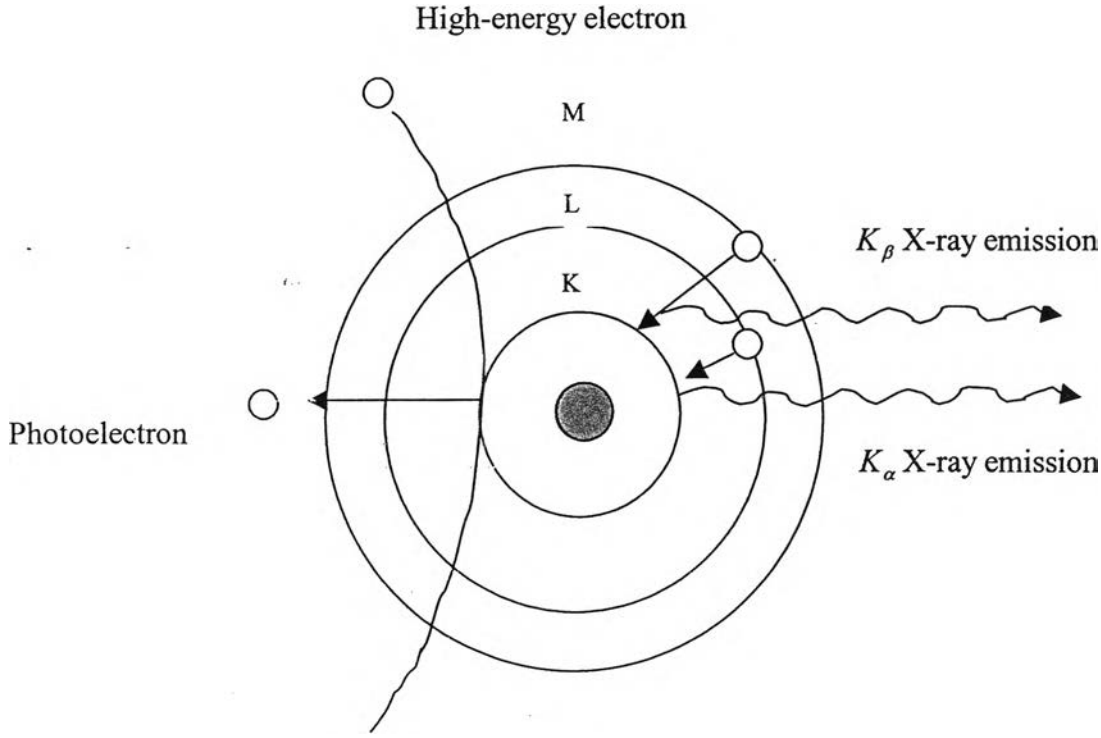

Figure 3.17: Schematic of the processes leading to the emission of characteristic X - ray

Lower atomic number elements have fewer X-ray peaks; in contrast, higher atomic number elements have more X- ray peaks. In the spectrum range of 0 – 20 keV, all elements from boron to uranium are detected. Therefore, characteristic X-ray lines in EDX method, which is a nondestructive technique, are used to identify the composition of the specimen. The weight or atomic percent of the specimen can be calculated from the area under the peaks. At first, the background noise in the EDX spectrum is subtracted. Then, the count rate is compared to the count rate of the reference sample.

$$k_i = \frac{I_i}{I_{ref}}, \qquad (3.12)$$

when k_l is the fraction of the count rate,

I_l is the count rate of sample with unknown composition,

I_{ref} is the count rate of sample with known composition,

index l is the element and transition concerned.

However, there are many factors that involve the calculation of composition in the sample. So, the real content or a better estimation is determined by multiplying k_l with some correction factors. These factors are called "ZAF correction"

So the real concentration C_l is

$$C_l = k_l ZAF\,, \qquad (3.13)$$

where $\boldsymbol{Z}$ is atomic number correction. This correction is used because of probabilities of backscattering in elements are different.

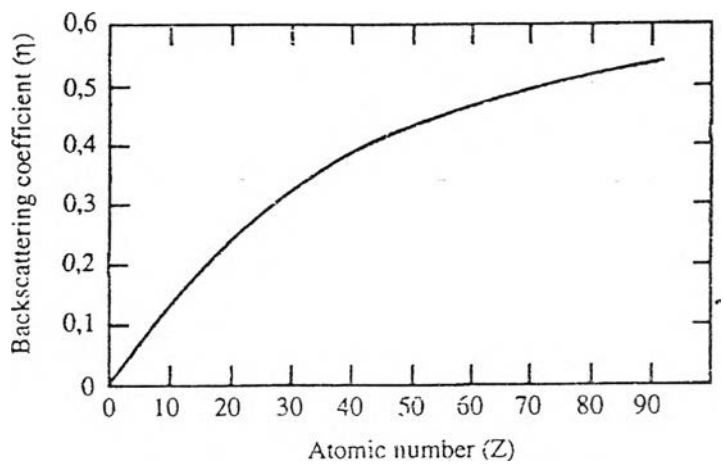

Figure 3.18: Backscattering coefficient dependence on the atomic number [38]

When the primary electrons bombard the specimen, some of electrons collide the atoms and make them ionize. Others are backscattered and X-rays are not

produced. Light elements (low z) have less effect for backscattering the primary electrons than heavy elements (high z) [38], as shown in Figure 3.18. On the other hand, the light elements have more ionization than the heavier elements. This is backscattered effect. This effect varies on accelerating voltage. So, the accelerating voltage should be constant in the specimen with unknown compositions and known compositions.

A is absorption dependent correction. Because X-ray radiation from different elements is generated in different depth in the sample, the absorption of radiation is varied. This factor is dependent on excitation volume size that depends on energy of the primary electrons and atomic number of the specimen. Furthermore, the absorption depends on an angle between the specimen surface and the primary electron beam.

F is secondary fluorescence correction. Continuous X-ray, which is produced in the specimen by the bombarding primary electrons, gives secondary fluorescence. The continuous X-ray can make the core electrons in the innermost shell eject from the atoms. The higher energy electrons can replace this vacancy. And then, the secondary fluorescence is produced. This factor depends on the composition in the excitation volume. For example, the composition of the sample is Ni and Fe. Ni has more atomic number than Fe. At first, Ni atoms generate the X-ray radiation when the primary electrons bombard the specimen. And then, Fe atoms absorb this X- ray and produce secondary fluorescence. As a result, X-ray intensity of Ni is decreased and X-ray intensity of Fe is increased.

The computer performs these ZAF corrections.